Petrology and geochemistry of the Neoproterozoic Nguba and Kundelungu Groups, Katangan Supergroup, southeast Congo: Implications for provenance, paleoweathering and geotectonic setting

M.J. Batumike [a,b,*], A.B. Kampunzu [c], J.H. Cailteux [d]

[a] Department of Geoscience, Shimane University, 1060 Nishikawatsu, Matsue, Shimane 690-8504, Japan
[b] Département de Géologie, Université de Lubumbashi, B.P. 1825, Lubumbashi, Congo
[c] Department of Geology, University of Botswana, Private Bag 0022, Gaborone, Botswana
[d] Département Recherche et Dévelopement, Group G. Forrest International, Lubumbashi, Congo

Abstract

The Nguba and Kundelungu Groups constitute the middle and upper parts of the Neoproterozoic Katangan Supergroup, respectively, and consist of conglomerates, sandstones, mudrocks and carbonates. During deposition, the Katangan basin received sediments originating from both northern and southern sources. The Nguba and Kundelungu Groups siliciclastic rocks have elemental abundances and ratios suggestive of a relatively felsic TTG source, although slightly more mafic compositions occur in the Nguba Group and the overlying "Petit Conglomérat" Formation at the base of the Kundelungu Group. Modal compositions of the Nguba Group rocks indicate a basement uplift provenance, and geochemical parameters indicate the source of both the Nguba and Kundelungu Groups had an active continental margin character.

Source area weathering was moderate in the Nguba Group. Low Chemical Index of Alteration (CIA) and Plagioclase Index of Alteration (PIA) indices and relatively uniform chemical compositions of the "Grand Conglomérat" and the "Petit Conglomérat" Formations lying respectively at the bases of the Nguba and Kundelungu Groups are compatible with deposition in a cool or frigid climate, and support their presumed petrographic based glaciogenic origin. High CIA and PIA indices in Upper Kalule rocks in the middle part of the Kundelungu Group point to the intensification of source weathering, possibly under tropical to subtropical climate under steady state conditions. Geochemical similarities between the Nguba Group and the "Petit Conglomérat" are compatible with a change from an extensional setting to compression, with derivation of the "Petit Conglomérat" by reworking of the underlying units during basin inversion. Change in provenance signatures and weathering indices in the Upper Kalule Formation may reflect reduced tectonism and resumption of supply of more weathered extrabasinal detritus, similar to that which fed the basal Roan Group.

Overall the data suggest derivation mainly from pre-Katangan Proterozoic sources with continental arc characteristics. The adjacent Paleoproterozoic Ubendian Belt, particularly the Bangweulu block calcalkaline plutonic and volcanic province, is a suitable candidate as the source for the Nguba and Kundelungu Group sedimentary rocks. However, Mesoproterozoic and Archaean terrains have also contributed a minor component to the basin.

Keywords: Sediment provenance; Geochemistry; Proterozoic; Katangan Supergroup; Congo

* Corresponding author. Present address: GEMOC, Department of Earth and Planetary Sciences, Macquarie University, NSW 2109, Sydney, Australia. Tel.: +61 2 9850 9676; fax: +61 2 9850 6904.

E-mail addresses: jbatumike@els.mq.edu.au, jbatumike@hotmail.com (M.J. Batumike).

1. Introduction

The Neoproterozoic Katangan Supergroup comprises an approximately 10 km thick succession of sedimentary rocks constituting the Katangan Belt located in the south-eastern part of the Democratic Republic of Congo (hereafter Congo), and extending southward into northwest Zambia (Fig. 1). Owing to its world-class stratiform Cu–Co deposits, this belt is also referred to as the Central Africa Copperbelt. The Katangan Supergroup is commonly subdivided into three groups: Roan Group, Nguba (formerly Lower Kundelungu) and Kundelungu (formerly Upper Kundelungu) Groups, in ascending stratigraphic order. This lithostratigraphic subdivision is based mainly on two diamictites/tillites well exposed throughout the region, forming regional stratigraphic markers (François, 1974, 1987, 1995; Cailteux et al., 1994; Cailteux, 2003).

Lithological associations of sedimentary rocks, their facies arrangements, and their detrital mineralogy and chemical composition can provide critical information on the tectonic, climatic and geochemical evolution of the continental crust, as they preserve the record of crust removed by erosion of the hinterland (e.g. Dickinson et al., 1983; Roser and Korsch, 1988; McLennan et al., 1993; Nesbitt et al., 1996). Many studies carried out on the Katangan Supergroup have focused on the famous stratiform Cu–Co mineralization hosted by the Roan Group succession (e.g. François, 1974; Cailteux, 1983; Cailteux et al., 1994; Wendorff, 2000).

In contrast, the Nguba and Kundelungu Groups were poorly investigated because of weak economic interest. The few geochemical studies carried out in these two groups were conducted in areas with Pb–Zn (Cu–Ge) deposits or occurrences such as Kipushi, Kengere and Lombe (e.g. Intiomale and Oosterbosch, 1974; Intiomale, 1982; Chabu, 1995) or with limestones exploited for cement and lime production, e.g. in Kakontwe (François, 1973). Moreover, most geochemical investigations carried out in the Katangan Supergroup were directed towards metallogenic questions (e.g. Intiomale and Oosterbosch, 1974; Intiomale, 1982; Cailteux, 1983; Chabu, 1995; Loris, 1996; Kampunzu et al., 2002a), and very few are sediment provenance studies (e.g. Kampunzu et al., 2002b).

This paper examines the modal compositions of sandstones from Nguba and Kundelungu Group rocks in the Katanga Province (S.E. Congo), and presents major and trace element data from conglomerate matrices, sandstones and mudrocks within these two groups. The focus of the study is on presenting the petrological and geochemical characteristics of these sedimentary rocks, and placing constraints on their source, tectonic setting, and the paleoclimatic environment in which they were deposited.

2. Geology

The Neoproterozoic Katangan Supergroup forms one of the Pan-African belt segments in sub-equatorial Africa. It is located between the Congo and the Kalahari cratons,

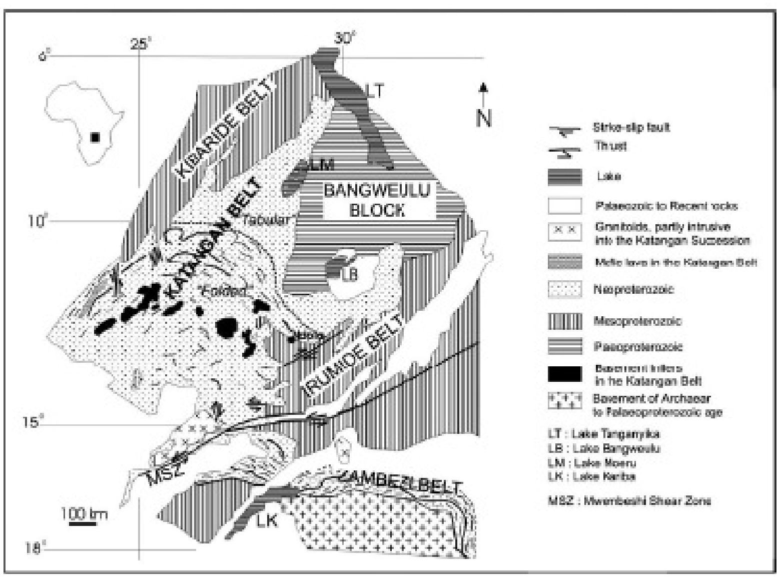

Fig. 1. The Katangan Belt and surrounding crustal blocks in central Africa, showing the tabular and folded Katangan (modified from Porada, 1989; Kampunzu and Cailteux, 1999).

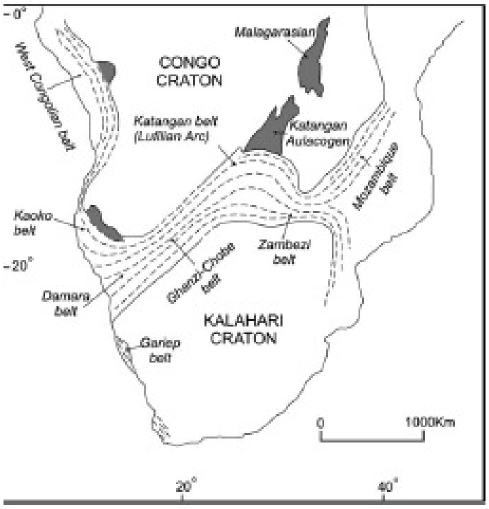

Fig. 2. Neoproterozoic belts (dashed lines) and major crustal blocks in south-central Africa (Kampunzu et al., 2000).

and extends from southern Katanga Province (S.E. Congo) to northwest Zambia (Figs. 1 and 2). The two diamictites that allow division of the Katangan Supergroup into three groups are the "Grand Conglomérat" and the "Petit Conglomérat", which lie at the bases of the Nguba and Kundelungu Groups, respectively (Fig. 3). These diamictites were correlated with the two worldwide Neoproterozoic glacials documented in detail by several workers (e.g. Young, 1995, 2002; Goddéris et al., 2003), and named the Sturtian or Rapitan (~750 Ma) and Varanger or Marinoan (~620 Ma) glacials. Geochronological data indicate deposition of the "Grand Conglomérat" at ca. 750 Ma (Kampunzu et al., 1998; Porada and Berhorst, 2000; Key et al., 2001; Master et al., 2002) supporting its correlation with the Sturtian glacial. In contrast, the age of the "Petit Conglomérat" is not yet constrained, and its correlation with the Marinoan glacial remains speculative.

The Roan Group is formed of clastic sedimentary rocks and carbonates (mainly dolomites and dolomitic shales). In contrast, the Nguba and Kundelungu Groups are mostly constituted of clastic sedimentary rocks with a main carbonate unit occurring in the Nguba Group named the Kakontwe Limestone. Roan Group rocks were deposited in a basin that evolved from a continental rift up to a proto-oceanic (Afar/Red-see type) rift (e.g. Kampunzu et al., 1993, 2000; Tembo et al., 1999). Mwashya Subgroup and Nguba Group rocks are assumed to have been deposited in a wide basin (Buffard, 1988; Cailteux et al., 1994) whereas the Kundelungu Group is taken to represent the inversion from extensional to compressional tectonics (Batumike et al., 2002; Kampunzu et al., 2003; John et al., 2004). The Plateaux Subgroup at the uppermost part of the Kundelungu Group is formed of subhorizontal rocks known only in the northern part of the Katangan belt.

3. Analytical methods

Representative samples of the clastic sedimentary rocks of the Nguba and Kundelungu Groups were collected from five localities (Kipushi, Luiswishi, Likasi, Tenke and Bunkeya) within the Lufilian Arc (Fig. 4). Following general petrographic description, modal compositions were determined for sandstones from the Upper Likasi Formation, the Monwezi Subgroup and the Plateaux Subgroup. Between 500 and 1000 points were counted on thin sections stained for both plagioclase and K-feldspar, using Gazzi–Dickinson methodology (Dickinson et al., 1983; Dickinson, 1985). Samples from other formations could not be counted due to their fine grain size or significant carbonate content.

Eighty-seven samples were selected for chemical analysis. These represent seven of the ten formations present. Samples collected from the Kakontwe Formation and the "Calcaire rose" were not analysed because they are carbonates and thus are not relevant for this study focused on clastic rocks. Samples were manually chipped to <1 cm, discarding any weathered rims. Large clasts were removed from the conglomerates in an attempt to analyze the matrix. The washed and dried chip was then crushed in a tungsten carbide ring mill for 30–50 s (Roser et al., 1998). Fine-grained samples weighing less than 50 g were powdered using an automatic agate pestle and mortar. After crushing, 10 g of each sample was dried for 24 h at 110 °C before conventional gravimetric determination of loss on ignition (LOI) by firing at 1000 °C for at least 2 h. Fusion beads for X-ray fluorescence analysis (XRF) were prepared using an alkali flux comprising 80% lithium tetraborate and 20% lithium metaborate with a sample to flux ratio of 1:2, following the method of Kimura and Yamada (1996). Major element and 14 trace elements abundances were analysed at Shimane University using a Rigaku RIX-2000 spectrometer equipped with a Rh-anode X-ray tube. Accuracy and precision of the method and results on some standard rocks are given in Kimura and Yamada (1996).

4. Petrography

The Nguba and Kundelungu Groups tillites are matrix-supported conglomerates, although clast-supported conglomeratic beds occur locally in the northern facies of the "Grand Conglomérat". Clasts are poorly sorted and include faceted and rounded to angular quartz, quartzite, granite, sandstones, shales, chert, dolomite, mafic igneous rocks, volcanic rocks and chlorite-sericite schist. Sandstones occur in the northern facies of the Nguba Group

Group	Subgroup	Formation	Lithologies
Kundelungu (Ku)	Plateaux Ku 3		Arkoses, with sandstones, sandy shales or conglomerate beds
	Kiubo Ku 2	Ku 2.2 Upper Kiubo	More or less dolomitic sandy shales or shales, rare impure limestones beds
		Ku 2.1 Lower Kiubo	Dolomitic siltstones, sandy shales or shales, feldspathic sandstones beds
	Kalule Ku 1	Ku 1.3 Upper Kalule	Dolomitic siltstones, sandy shales or shales, pink oolitic limestone (base)
		Ku 1.2 Middle Kalule	Siltstones, marly and sandy shales, pink dolomite ("Calacaire rose")
		Ku 1.1 (Lower Kal.) Petit Conglomerat	Diamictite
Nguba (Ng)	Monwezi Ng 2		More or less dolomitic siltstones or sandy shales and shales, sandstones
	Likasi Ng 1	Ng 1.3 Upper Likasi	Slightly dolomitic arkosic siltstones, sandy shales and shales, sandstones
		Ng 1.2 Middle Likasi	Dolomites/limestones ("Kakontwe Limestone") shales and sandy shales
		Ng 1.1 (Lower Likasi) Grand Conglomerat	Diamictite
Roan (R)	Mwanshya R 4	Upper M. R 4.2	Shales, carbonaceous shales and sandstones
		Lower M. R 4.1	Dolomites, jasper, pyroclastics and hematite
	Dipeta R 3	R 3.4	Dolomites interbedded with shales
		R 3.3	Dolomitic siltstones and feldspathic sandstones
		R 3.2	Doleritic and gabbroic bodies
		R 3.1 "R.G.S"	Dolomitic siltstones
	Mines R 2	R 2.3 Kambove	Laminated, stromatolitic, talcose dolomites and dolomitic siltstones
		R 2.2 Dolomitic Shale	Dolomitic and carbonaceous shales, dolomite, sandy dolomite, sandstones and arkoses
		R 2.1 Kamoto	R 2.1.3 R.S.C (Roches Siliceuses Cellulaires) stromatolitic dolomite
			R 2.1.2 Bedded dolomites and siltstones, silty dolomite
			R 2.1.1 grey R.A.T (Roches Argilo-talqueuses) dolomitic siltstones
	R.A.T R 1	R 1.3	Pink-lilac chloritic dolomitic siltstones
		R 1.2	Chloritic silt, stromatolitic dolomite, sandstones
		R 1.1	Hematitic, slightly dolomitic siltstones
Kibaran and pre-Kibaran			

Fig. 3. Stratigraphy of the Katangan Supergroup in southern Katanga. Modified from François (1974, 1987), Porada and Berhorst (2000) and Cailteux (2003). The names Upper Kalule, Middle Kalule, Upper Likasi and Middle Likasi are used informally, for Ku1.3, Ku1.2, Ng1.3, and Ng1.2, respectively.

(Bunkeya area, Fig. 4) and in the top part of the Kundelungu Group (Plateaux Subgroup), their compositions are presented in the next section.

The Nguba Group siliciclastic rocks are characterized by a decrease in grain size from north to south. Sandstones and siltstones occur in the northern regions (e.g. Bunkeya area, Fig. 4) whereas shales are abundant in the southern regions (e.g. Kipushi, Fig. 4), where carbonates are also well developed. The "Petit Conglomérat" matrix in the northern region is sandy and feldspathic clasts are more abundant (~13 vol.%, Bunkeya area) than in the southern region, where the matrix is muddier and feldspar clasts comprise ~2 vol.%. Volcanic rock clasts observed in this formation in the north are absent in the south. The thickness of Kundelungu Group formations overlying the "Petit Conglomérat" also increases southward. The Middle Kalule Formation (Ku 1.2) is 300 m thick in the northern region (Bunkeya, Fig. 4) and up to 1600 m in the south (e.g. Luiswishi, Fig. 4).

5. Sandstones composition and tectonic setting

Sandstone detrital modes are useful for constraining provenance and tectonic setting (e.g. Dickinson and Suczek, 1979; Dickinson et al., 1983), provided no large-scale replacement of feldspar and rock fragments or no diagenetic feldspar have occurred. Detrital modes of representative sandstones from the Nguba and Kundelungu Groups are given in Table 1. Nguba Group sandstones are medium- to fine-grained and typically poorly sorted. They are cemented by calcite and clay minerals. The rocks are massive to finely bedded, and locally exhibit unidirectional cross bedding. Ranges of modal compositions in Upper Likasi Formation and Monwezi Subgroup sandstones are $Q_{47-76}F_{21-45}L_{0-32}$ and $Q_{45-61}F_{38-53}L_{0-5}$ respectively (Table 1). K-feldspar content increases from Upper Likasi to Monwezi Subgroup sandstones, whereas lithic fragment content decreases. The main lithic fragments comprise volcanic rocks, quartzites, sandstones, granitoids,

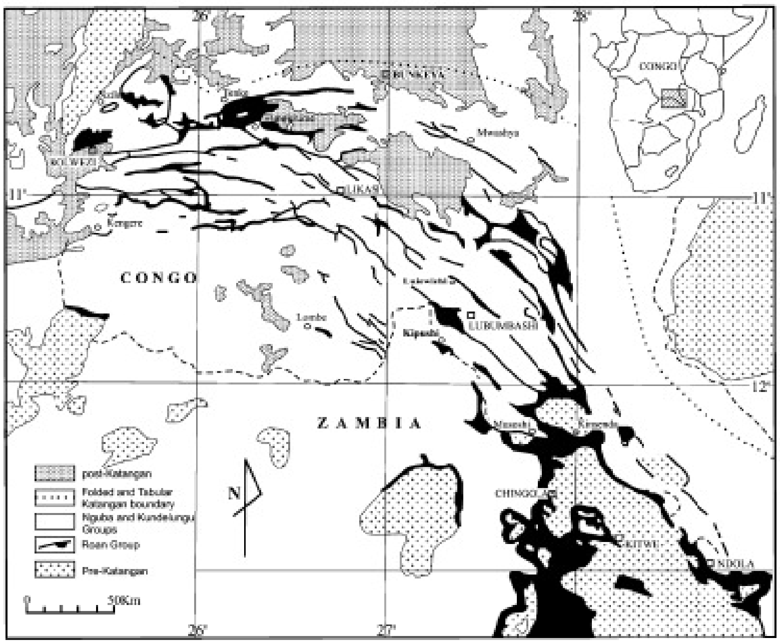

Fig. 4. Locality and division of the Katangan belt, with main localities including the study areas. Modified from Cailteux et al. (1994).

and chlorite–sericite schists. Feldspars are generally well preserved, but partial conversion to carbonates or clays occur in places. However, such replacements do not affect the detrital modes significantly. Apatite and zircon are the most common detrital heavy minerals.

The Plateaux Subgroup sandstones examined here were collected in the Tenke area. They are not the typical facies of the subgroup, and thus conclusions based on these samples are limited to this area only. Additional samples are needed, especially from the extreme northern region of the Katangan belt, for fuller characterization of the Plateaux Subgroup. The sandstones examined here are quartz arenites, with compositions in the range $Q_{95-99}F_{1-2}L_{1-3}$. They are mostly well-sorted sandstones containing well-rounded quartz grains cemented by diagenetic silica, but hematite and clay cements occur locally. Secondary silica overgrowths occur around quartz grains. Zircons are rare, and lithic clasts are of (meta)sedimentary rocks. Nguba and Kundelungu Group siltstones and shales vary from finely bedded to massive, and range from greenish gray to reddish gray. Siltstones locally show unidirectional cross bedding, and shales may contain wavy beds.

Q_tFL and Q_mFL_t diagrams (Fig. 5) show that Upper Likasi Formation sandstones fall in the recycled orogen, transitional continental, and basement uplift fields, whereas Monwezi Subgroup sandstones are confined to the basement uplift domain. Abundances of volcanic and (meta)sedimentary lithic fragments decrease upward from the Upper Likasi Formation to the Monwezi Subgroup. Although there is wide variation in lithic volcanic/total lithic (Lv/L) ratios in the Upper Likasi suite, but these ratios (0.1–1.0, Table 1) seem greater than those in the Monwezi Subgroup (0–0.54, Table 1), which also shows less variation. Similarly, feldspar content in the Monwezi Subgroup increases over the Upper Likasi Formation, and the plagioclase/total feldspar (P/F) ratio decreases to an average of 0.67 (Table 1). These patterns are compatible with uplift and erosion causing exposure of an increasing proportion of plutonic rocks in the source, possibly the roots of a volcanic province.

All samples from the Plateaux Subgroup fall in the craton interior (Fig. 5(a)) and quartzose-recycled domains (Fig. 5(b)). Dickinson et al. (1983) considered sandstones plotting in this field as mature and derived from relatively low-lying granitoid sources, supplemented by recycled sands from associated platform or passive margin basins.

6. Geochemistry

The Nguba and Kundelungu sedimentary rocks display diverse chemical compositions. Analyses of the samples are given in Table 2. The major element data for each sample

Table 1
Detrital modal compositions of Nguba and Kundelungu Group sandstones

Sample	Qm	Qp	P	K	Lv	Lsm	Matrix	Total	Q%	F%	L%	P/F	Lv/L
Plateaux Subgroup (Ku 3)													
B 06	74.6	9.4	0.4	1.4	0.0	3.0	11.2	100.0	94.6	2.0	3.4	0.20	0.00
B 07	80.3	10.5	0.7	1.3	0.0	0.7	6.5	100.0	97.0	2.2	0.8	0.36	0.00
B 09A	87.0	7.0	0.0	0.6	0.0	0.8	4.6	100.0	98.6	0.6	0.8	0.00	0.00
B 09C	77.8	12.4	0.0	1.1	0.0	2.8	5.8	100.0	95.8	1.2	3.0	0.00	0.00
B 10A	75.4	17.3	0.2	0.6	0.0	2.7	3.8	100.0	96.4	0.8	2.8	0.25	0.00
B 16	75.2	11.6	0.0	1.4	0.0	2.4	9.4	100.0	95.8	1.6	2.6	0.00	0.00
Average	78.4	11.4	0.2	1.1	0.0	2.1	6.9		96.4	1.4	2.2	0.14	0.00
STDEV	4.7	3.4	0.3	0.4	0.0	1.0	2.9		1.4	0.6	1.1	0.16	0.00
Monwezi Subgroup (Ng 2)													
JB 140	43.2	2.4	24.4	16.2	1.4	1.2	11.2	100.0	51.4	45.7	2.9	0.60	0.54
JB 139	52.9	0.3	25.9	14.1	0.7	0.9	5.3	100.0	56.1	42.2	1.7	0.65	0.42
JB 138	44.5	2.3	25.2	15.6	1.5	2.2	8.7	100.0	51.3	44.7	4.1	0.62	0.42
JB 137	45.6	1.1	22.2	13.1	1.0	2.8	14.1	100.0	54.5	41.1	4.4	0.63	0.26
JB 136	43.8	2.9	23.3	15.7	0.8	1.8	11.7	100.0	52.9	44.2	2.9	0.60	0.31
JB 135	43.6	1.4	31.9	11.7	0.4	2.5	8.4	100.0	49.1	47.6	3.2	0.73	0.13
JB 134	40.3	3.9	23.2	12.5	0.9	3.2	16.0	100.0	52.7	42.5	4.9	0.65	0.22
JB 132	45.4	4.2	23.0	8.7	0.3	1.3	17.0	100.0	59.8	38.2	2.0	0.73	0.20
JB 131	53.0	0.6	27.5	6.6	0.2	2.1	10.1	100.0	59.6	37.8	2.6	0.81	0.08
BK 06A	47.2	6.7	22.6	11.3	0.0	0.6	11.5	100.0	61.0	38.3	0.7	0.67	0.00
BK 06B	40.2	4.4	30.9	10.1	0.4	1.0	13.0	100.0	51.3	47.1	1.6	0.75	0.29
BK 06C	38.2	3.7	29.1	17.7	0.2	0.6	10.6	100.0	46.8	52.4	0.9	0.62	0.25
BK 05	35.1	5.8	32.1	15.1	0.0	0.2	11.8	100.0	46.3	53.5	0.2	0.68	0.00
BK 04	34.6	4.6	30.9	15.1	0.2	1.0	13.5	100.0	45.4	53.2	1.3	0.67	0.17
Average	43.4	3.2	26.6	13.1	0.6	1.5	11.6	100.0	52.7	44.9	2.4	0.67	0.23
STDEV	5.6	1.9	3.7	3.2	0.5	0.9	3.1		5.0	5.4	1.4	0.06	0.16
Upper Likasi Formation (Ng 1.3)													
JB 128	52.3	2.3	16.0	4.0	0.4	3.1	21.9	100.0	70.0	25.6	4.4	0.80	0.11
JB 127	54.6	5.2	13.7	2.6	0.0	3.0	21.0	100.0	75.7	20.6	3.7	0.84	0.00
JB 127B	47.3	7.3	15.8	2.6	0.0	2.6	24.3	100.0	72.1	24.4	3.5	0.86	0.00
JB 126B	49.8	3.4	23.3	3.2	3.0	1.1	16.1	100.0	63.5	31.6	4.9	0.88	0.74
JB 125B	50.1	1.1	21.6	4.5	3.8	0.8	18.2	100.0	62.6	31.9	5.5	0.83	0.83
JB 125B	43.7	1.6	22.1	2.4	3.2	1.8	25.2	100.0	60.6	32.7	6.6	0.90	0.64
JB 124	49.3	1.3	16.3	3.3	2.2	1.1	26.6	100.0	68.8	26.7	4.5	0.83	0.67
JB 124B	49.7	0.6	19.8	4.3	2.9	0.8	21.9	100.0	64.4	30.8	4.8	0.82	0.79
JB 123	42.1	1.5	25.9	4.4	0.0	1.7	24.4	100.0	57.7	40.1	2.3	0.86	0.00
JB 122	44.7	2.7	22.4	5.1	2.5	0.0	22.6	100.0	61.2	35.6	3.2	0.81	1.00
JB 121	42.5	3.9	29.1	4.1	0.4	0.0	19.9	100.0	58.0	41.5	0.5	0.88	1.00
JB 120	40.3	1.8	30.4	4.6	0.0	0.0	23.0	100.0	54.6	45.4	0.0	0.87	–
BK 03B	36.3	2.0	19.3	2.6	10.9	8.4	20.3	100.0	48.2	27.6	24.3	0.88	0.56
BK 03B′	35.4	4.2	24.5	2.1	9.2	8.9	15.8	100.0	47.0	31.5	21.4	0.92	0.51
Average	45.6	2.8	21.4	3.6	2.7	2.4	21.5	100.0	61.7	31.9	6.4	0.86	0.53
STDEV	5.8	1.9	5.0	1.0	3.4	2.9	3.2		8.4	7.0	7.2	0.03	0.38

were recalculated to 100% after deduction of loss on ignition, for all comparisons given below and for plotting. The same normalisation factors were also applied to the trace element data for each sample.

6.1. Major elements

In the Nguba Group, the "Grand Conglomérat" matrix samples have a restricted range in anhydrous SiO_2 (62.2–66.8 wt%) and Al_2O_3 (3.4–16.1 wt%) abundances when sample JB58 is excluded. High Fe_2O_3t content (18.04 wt%) in this sample acts as a diluent for the other major elements. The "Grand Conglomérat" samples have greater TiO_2 and MgO relative to the overlying formations. The Upper Likasi samples are mainly siltstones and mudstones (Table 2). Samples from the Kipushi area (Table 2) have relatively low silica contents (59.2–62.0 wt%). Those from the Bunkeya area (samples JB33 and JB38, Table 2) have similar TiO_2 contents (1.9 and 1.8 wt%, respectively) to the "Grand Conglomérat" matrix.

The Monwezi Subgroup is represented by five sandstones and six mudrocks (Table 2). The sandstones have higher SiO_2 and lower Al_2O_3 contents (69.9–78.5 and 8.6–10.0 wt% respectively) compared to the mudrocks (SiO_2: 57.4–65.1 wt% and Al_2O_3: 10.9–17.2 wt%). Fractionation between sand and mud via sorting is thus the most significant amongst the formations analysed. Consequently, the mudrocks also have greater TiO_2, Fe_2O_3t and MgO contents than most of the sandstones (Fig. 6). The mudrocks also tend to have greater K_2O, but lesser

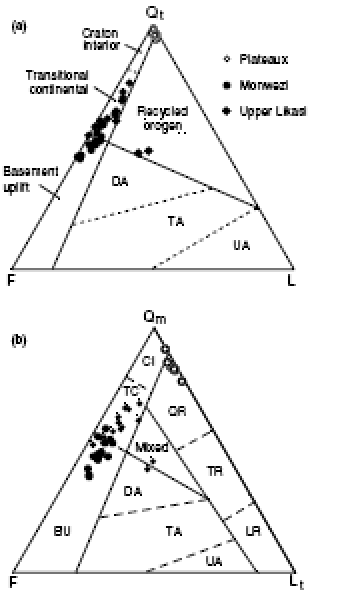

Fig. 5. (a) Q_tFL and (b) Q_mFL_t diagrams for Nguba and Kundelungu Group sandstones, after Dickinson et al. (1983). Abbreviations used are UA: undissected arc; TA: transitional arc; DA: dissected arc; CI: craton interior; TC: transitional continental; BU: basement uplift; QR: quartzose recycled; TR: transitional recycled; LR: lithic recycled.

Na_2O (Fig. 6). This is consistent with greater proportions of quartz, feldspar and lithic fragments in the sandstones versus aluminous clays in the mudrocks.

The "Petit Conglomérat" samples show relatively narrow range content in anhydrous Al_2O_3 (12.0–15.7 wt%), SiO_2 (60.0–67.0 wt%) and K_2O (2.6–3.9 wt%). Samples from the northern areas (Bunkeya and Tenke, Fig. 4) have lower Al_2O_3, CaO and MgO contents, and greater SiO_2 and Na_2O than those from Likasi, Luiswishi and Kipushi (Table 2, Fig. 7). This is possibly linked to the nature of the matrix that is sandy to the north and muddier in the south, and the abundance of plagioclase clasts in the north but few to the south. Almost all Upper Kalule Formation (Ku 1.3) siltstones and mudstones have greater K_2O (4.5–7.3 wt%, Table 2) than those from other formations within the succession (Table 2). All Plateaux Subgroup sandstones are highly enriched in silica (>98 wt%) and hence are strongly depleted in all other oxides compared to the underlying units.

6.2. Trace elements

Among the trace element analysed, seven (Ba, Ce, Pb, Th, Y, Zr, and Sr) show relatively poor correlation with Al_2O_3. Very high values of Ba (>1000 ppm) are seen in a few Monwezi Group, "Petit Conglomérat" and Middle Kalule samples from Bunkeya. This is possibly due to the presence of barite as postulated by Bellière (1966). Ce, Pb and Y abundances show no correlation with Al_2O_3 and no clear differences between formations. The behavior of Zr (no correlation with Al_2O_3) is common in sedimentary suites, due to primary control by detrital zircon abundances. Plateaux Group sandstones have variable but significant Zr contents (46–130 ppm), compared to their very low Ba, Ce, Th, and Y contents (Table 2). Most samples contain <200 ppm of Sr, but Middle Kalule Formation samples with elevated CaO contents have abundances >200 ppm. This reflects the association of these two elements with the carbonate fraction.

The remaining trace elements (Ga, Nb, Sc, Rb, Cr, Ni, and V) show positive correlations with Al_2O_3 of varying strength, suggesting their abundances are mainly controlled by the clay fraction and sorting. The matrix samples from the "Grand Conglomérat", have high Nb content (40 ppm). Several of these enriched samples also contain higher values of TiO_2, with which Nb is geochemically coherent.

Cr, Ni and V display a common pattern with two intersecting trends (Fig. 8). Two different trend are observed, samples from the lower part of the succession (LP trend; Nguba Group and the "Petit Conglomérat") show different trend relative to those from the upper part (UP trend, Middle and Upper Kalule). This grouping of elements suggests a compositional change on the source region. The Nguba Group and the "Petit Conglomérat" had then a somewhat more mafic source than the Middle and Upper Kalule Formations as shown by the relatively great content in these elements in the lower part of the succession. This is also reflected by similar but less pronounced contrasts in TiO_2 and Sc.

7. Discussion

7.1. Tectonic setting

As noted above, detrital modal compositions of the Upper Likasi Formation and Monwezi Subgroup sandstones indicate that they had recycled orogen to basement uplift provenances, whilst the Plateaux Subgroup samples have the characteristics of craton interior and quartzose recycled sandstones (Fig. 5). According to Dickinson (1985), orogenic recycling may occur in subduction complexes, backarc thrust belts, and in suture zones. Samples falling in the basement uplift field generally reflect continental rift or foreland basins setting in which the sedimentary materials are rapidly eroded, transported and buried, so that feldspars (especially plagioclase) are well preserved

Table 2
Major and trace element analyses of Nguba and Kundelungu Group rocks (hydrous basis). Major elements wt%, trace elements ppm

SaNr	Lith	Loc	SiO_2	TiO_2	Al_2O_3	Fe_2O_3	MnO	MgO	CaO	Na_2O	K_2O	P_2O_5	LOI	Total	Ba	Ce	Cr	Ga	Nb	Ni	Pb	Rb	Sc	Sr	Th	V	Y	Zr
Kundelungu Group																												
Plateaux Subgroup (Ku 3)																												
JB14	F msv sst	Tnk	98.25	0.05	0.43	0.25	0.00	0.01	0.10	0.07	0.02	0.01	0.45	99.68	104	12	1	2	1	<1	7	4	<1	4	0.4	<1	2	108
JB20	F msv sst	Tnk	96.43	0.02	0.33	0.04	0.00	0.01	0.05	0.04	0.04	0.01	0.17	97.12	<5	16	<1	<1	1	<1	3	6	<1	4	1.5	<1	2	44
JB39	Crs msv sst	Tnk	97.90	0.05	0.64	0.95	0.00	0.02	0.01	0.13	0.01	0.01	0.51	100.31	641	1	3	2	2	<1	5	9	<1	13	0.5	<1	3	82
JB34	F msv sst	Tnk	97.84	0.05	1.17	0.33	0.00	0.02	0.05	0.06	0.18	0.01	0.58	100.23	118	11	5	2	1	<1	5	3	<1	4	0.2	41	2	129
JB44	Crs msv sst	Tnk	97.85	0.06	1.04	0.23	0.00	0.02	0.05	0.09	0.11	0.01	0.45	99.95	29	20	<1	2	2	<1	5	7	1.2	4	0.5	4	4	79
JB45	F msv sst	Tnk	94.45	0.02	0.53	0.15	0.00	0.01	0.06	0.12	0.07	0.01	0.22	95.68	14	12	<1	2	1	<1	3	6	<1	4	0.8	<1	4	47
Upper Kafubu Formation (Ku 1.3)																												
JB29	Lam slt	Lsw	53.45	0.82	15.28	6.80	0.07	4.81	4.18	0.14	5.67	0.17	7.91	99.35	462	37	71	23	14	42	6	188	15.5	47	9.3	120	34	192
JB1	Lam slt	Lsw	61.16	0.80	16.30	7.02	0.14	3.22	0.32	0.14	3.90	0.29	3.80	99.05	399	37	93	24	13	49	2	190	19.6	17	11.9	139	37	168
JB3	Lam slt	Lsw	63.70	0.82	15.41	6.14	0.10	3.35	0.40	0.18	5.53	0.22	3.61	99.46	571	32	66	23	13	35	4	189	17.8	15	9.7	142	34	177
JB4	Msv slt	Lsw	63.65	0.85	14.52	7.53	0.13	3.46	0.36	0.08	5.07	0.26	3.48	99.35	641	44	75	22	14	40	3	168	13.4	13	11.1	124	37	233
JB5	Lam mst	Lsw	64.75	0.88	16.76	7.02	0.02	1.13	0.05	0.09	5.04	0.18	3.91	99.77	800	56	86	24	16	36	4	166	14.4	21	11.3	123	64	236
JB6	Msv slt	Lsw	64.72	0.78	15.15	6.12	0.14	2.07	0.29	0.09	5.61	0.23	3.40	99.35	674	36	73	22	12	33	1	185	14.8	15	8.9	129	31	147
JB9	Lam slt	Lsw	67.17	0.72	13.39	6.40	0.08	3.22	0.35	0.13	4.31	0.22	3.32	99.32	555	49	64	18	11	40	3	139	15.2	14	8.0	119	31	164
JB10	Lam mst	Lsw	52.86	0.76	16.78	6.90	0.09	4.49	7.29	0.12	6.62	0.17	3.51	99.59	537	17	86	26	12	43	11	230	18.3	71	7.2	165	34	132
JB15	Msv slt	Lsw	53.20	0.71	14.29	6.22	0.11	5.19	5.38	0.09	5.00	0.18	9.38	99.73	417	49	63	22	12	39	3	155	15.1	55	9.1	111	28	140
JB16	Msv slt	Lsw	55.05	0.99	19.22	7.90	0.02	4.07	0.61	0.13	6.81	0.18	4.48	100.26	601	18	102	32	16	54	5	238	20.5	21	7.1	192	30	113
JB2	Lam slt	Lsw	65.07	0.78	14.79	6.48	0.06	2.56	0.38	0.15	5.21	0.31	3.27	99.35	562	61	71	23	13	33	2	171	14.0	16	22.5	129	35	167
JB8	Msv slt	Lsw	64.67	0.69	13.84	7.61	0.13	3.81	0.35	0.06	4.45	0.19	3.48	99.25	605	73	68	21	11	41	5	148	10.7	18	8.5	114	29	171
JB11	Lam slt	Lsw	68.64	0.60	13.46	5.72	0.05	2.70	0.29	0.15	4.55	0.19	2.58	99.35	485	37	51	19	10	31	5	138	11.7	10	6.3	91	29	166
JB12	Lam slt	Lsw	56.35	0.89	15.18	6.85	0.05	4.38	3.45	0.40	5.45	0.22	6.48	99.36	453	35	70	23	14	37	4	181	15.3	44	8.8	127	36	238
JB99	Msv slt	Lsw	56.55	0.87	18.79	8.83	0.03	3.80	0.23	0.12	7.04	0.18	4.19	100.65	575	24	108	23	15	50	4	228	22.0	15	16.7	207	36	173
JB100	Msv slt	Lsw	58.81	0.92	16.28	7.89	0.03	3.85	0.37	0.08	5.96	0.26	3.86	98.29	495	87	92	20	16	44	4	185	15.8	17	16.0	173	36	215
JB22	Lam slt	Bky	57.42	0.83	12.01	4.94	0.06	2.74	6.58	2.73	3.36	0.22	8.06	98.91	301	92	71	16	13	24	8	108	11.9	86	13.8	103	45	246
JB37	Lam slt	Bky	54.96	0.70	10.52	4.33	0.09	3.58	8.47	2.40	3.21	0.20	10.26	98.65	256	91	50	14	11	23	5	95	11.8	78	11.3	88	41	220
Middle Kafubu Formation (Ku 1.2)																												
JB31	Lam mst	Bky	26.98	0.40	6.41	4.03	0.13	1.74	31.51	1.09	1.60	0.09	25.21	99.19	114	41	44	9	6	24	7	53	6.8	264	7.3	51	19	73
JB32	Lam slt	Tnk	35.92	0.55	8.78	5.07	0.07	2.71	22.13	1.81	2.03	0.18	19.61	98.81	177	50	50	13	8	30	4	71	10.4	341	9.1	85	21	98
JB33	Lam slt	Bky	29.25	0.42	5.24	2.86	0.07	1.59	30.97	1.45	0.95	0.11	25.11	98.01	303	34	32	8	6	16	5	33	5.6	440	6.3	46	21	91
JB19	Lam mst	Bky	41.87	0.65	11.64	6.27	0.09	2.60	16.40	1.34	2.89	0.18	15.00	98.88	236	55	68	17	10	43	12	102	11.7	195	10.2	105	26	119
JB23	Msv slt	Tnk	36.34	0.55	8.37	4.43	0.07	3.10	22.02	1.88	1.85	0.18	20.06	98.76	169	48	48	13	8	26	6	66	10.8	310	8.6	84	23	102
JB41	Lam mst	Tnk	40.47	0.60	9.85	4.51	0.06	2.71	17.65	2.44	1.65	0.18	17.41	98.42	258	48	53	13	8	30	5	66	12.7	166	8.1	66	28	128
JB43	Lam slt	Bky	40.12	0.57	7.04	3.57	0.05	1.86	22.25	2.04	1.15	0.18	19.02	97.83	321	55	41	10	9	21	7	45	8.9	368	9.8	58	25	168
JB49	Lam mst	Tnk	48.78	0.49	10.67	5.18	0.06	3.10	12.66	2.17	2.06	0.18	15.01	98.62	416	63	60	15	10	34	5	80	13.5	181	9.5	104	29	152
JB50	Lam slt	Tnk	34.43	0.48	5.46	3.30	0.07	2.60	26.02	1.71	0.89	0.18	22.78	97.87	1273	28	37	7	7	16	4	33	5.8	395	7.8	41	23	132
JB86	Msv slt	Kps	55.92	0.88	10.47	4.95	0.10	2.76	8.48	2.56	1.87	0.23	10.23	98.45	326	92	72	13	14	24	4	80	12.0	135	13.6	111	41	313
JB87	Msv slt	Kps	54.32	0.76	15.73	6.80	0.06	3.47	4.06	1.90	3.81	0.18	7.75	99.62	589	62	73	18	14	45	4	159	16.8	110	15.3	154	33	162
JB88	Msv slt	Kps	55.20	0.85	18.24	7.71	0.04	3.71	2.15	2.13	4.22	0.20	5.95	100.39	828	69	107	25	15	51	4	165	19.4	59	13.3	210	38	180
JB90	Msv slt	Kps	58.00	0.76	11.19	5.21	0.09	2.84	7.05	2.69	1.71	0.20	8.66	98.41	314	65	69	14	12	32	4	74	11.9	176	9.7	127	36	200
JB91	Msv slt	Kps	56.91	0.90	15.25	6.52	0.14	4.07	7.05	2.09	4.55	0.22	0.68	98.38	718	140	96	19	15	71	4	196	18.7	106	16.1	158	38	195
JB92	Msv slt	Kps	57.16	0.79	10.19	5.13	0.11	2.86	8.06	2.25	1.84	0.21	9.62	98.19	346	84	62	12	14	35	5	82	11.5	167	12.6	106	37	260
JB94	Msv slt	Lks	55.25	0.73	12.02	6.11	0.12	3.29	7.28	2.40	1.85	0.19	9.11	98.39	314	53	68	13	12	39	4	77	13.5	134	11.4	123	30	158
JB95	Msv slt	Lks	57.00	0.74	12.52	5.99	0.08	3.13	6.39	2.09	2.17	0.18	8.27	98.58	388	59	77	9	13	41	7	89	14.0	137	15.8	131	33	164
JB97	Msv slt	Lsw	61.47	0.80	10.74	4.24	0.10	2.40	3.71	3.23	2.63	0.19	7.31	98.27	329	76	47	12	14	23	3	81	11.3	96	13.6	87	40	302
JB98	Msv slt	Lsw	61.70	0.89	11.37	5.24	0.09	2.61	4.79	3.15	2.04	0.22	6.38	98.49	207	110	79	12	16	28	4	80	10.8	96	16.2	119	44	374
Petit Conglomerat (Ku 1.1)																												
JB18	Crs msv sst	Tnk	61.16	0.86	12.07	8.80	0.09	3.09	2.78	1.81	3.11	0.32	4.81	98.90	405	78	71	17	19	40	12	117	18.3	59	10.3	143	34	194
JB25	Crs msv sst	Tnk	64.36	0.78	11.33	7.14	0.10	2.79	2.55	1.70	3.08	0.22	4.99	99.05	357	70	59	16	19	31	10	116	15.2	49	10.7	114	26	204
JB27	Crs msv sst	Tnk	64.07	0.81	11.72	7.22	0.08	2.76	2.35	1.84	3.12	0.25	5.06	99.20	400	74	63	17	19	30	11	115	13.7	51	10.4	114	27	206
JB30	Crs msv sst	Tnk	60.59	0.96	12.56	8.79	0.09	2.96	2.88	2.17	3.08	0.36	4.98	99.35	317	69	73	18	22	36	10	114	19.0	58	10.8	163	30	207
JB40	F msv sst	Bky	61.59	0.67	10.64	5.26	0.10	1.91	6.85	2.03	2.49	0.14	6.58	98.67	506	55	69	14	10	32	10	85	12.4	137	7.1	112	24	146
JB42	F msv sst	Bky	60.75	0.68	10.24	5.31	0.09	1.87	4.84	1.89	2.66	0.14	5.67	94.13	463	56	67	14	9	33	10	88	11.4	118	7.3	113	22	146
JB47	Crs msv sst	Tnk	60.46	0.58	12.55	9.65	0.08	3.21	2.37	2.37	2.62	0.37	4.78	99.45	352	73	83	18	19	39	9	96	20.7	48	8.9	172	30	191
JB48	F msv sst	Bky	60.64	0.68	10.54	5.26	0.11	1.98	7.49	2.09	2.40	0.14	7.48	98.72	420	54	63	14	10	31	9	82	12.8	135	7.5	110	24	152
JB75	Crs msv sst	Kps	58.96	0.80	14.23	6.84	0.08	3.78	2.76	1.36	3.69	0.19	6.18	98.80	970	56	96	19	14	58	4	137	18.2	58	10.5	191	35	192
JB76	Vf msv sst	Kps	57.84	0.82	14.54	6.89	0.08	3.17	3.87	1.64	3.56	0.20	6.23	98.83	720	57	104	20	14	57	4	126	17.8	87	10.2	200	35	195
JB77	Vf msv sst	Kps	56.31	0.79	13.94	6.91	0.09	3.26	5.06	1.59	3.38	0.19	7.25	98.73	602	47	105	18	13	56	4	118	16.4	108	9.6	186	33	176
JB78	Vf msv sst	Kps	55.51	0.76	12.85	6.47	0.11	3.11	6.38	1.63	3.15	0.18	8.77	98.47	639	57	86	17	9	50	4	111	14.6	138	9.2	166	29	177
JB79	Vf msv sst	Kps	54.95	0.74	12.99	6.83	0.11	3.19	6.16	1.60	3.33	0.17	8.55	98.62	642	49	91	15	12	51	4	116	16.6	113	10.6	174	30	165
JB80	Vf msv sst	Kps	57.25	0.78	13.64	6.40	0.09	3.07	4.56	1.71	3.40	0.18	7.41	98.88	715	49	90	17	13	51	4	117	15.2	102	9.2	183	31	182
JB81	Vf-f msv sst	Lks	56.38	0.78	14.09	6.98	0.08	3.08	5.14	1.63	3.52	0.18	7.15	99.02	798	55	91	18	13	54	4	125	16.9	108	9.6	182	35	182
JB83	Vf msv sst- mst	Lks	53.63	0.73	12.38	5.91	0.09	3.91	7.51	1.50	3.05	0.18	9.62	98.52	421	70	86	15	12	50	8	108	15.2	125	9.6	147	29	195
JB84	Msv slt	Lsw	54.87	0.73	13.15	6.62	0.09	3.66	6.80	1.44	3.11	0.18	8.59	98.62	574	61	85	16	14	56	6	112	14.8	135	10.1	154	44	172
JB85	Msv slt	Lsw	55.23	0.74	13.33	6.66	0.08	2.95	6.61	1.58	3.14	0.18	8.25	98.75	603	65	89	15	12	61	5	112	15.2	129	10.5	156	35	171
Nguba Group																												
Monwezi Subgroup (Ng 2)																												
JB15	F msv sst	Bky	77.45	0.38	8.88	3.13	0.03	0.95	1.80	3.98	1.98	0.08	0.29	98.96	583	33	24	10	6	11	4	47	6.6	77	4.6	61	17	94
JB16	F msv sst	Bky	75.29	0.48	9.34	2.94	0.07	0.75	1.62	4.08	1.96	0.09	2.51	99.14	1507	26	37	10	8	18	5	48	6.8	85	5.2	68	24	102
JB21	F msv sst	Bky	63.61	0.82	7.82	5.45	0.12	1.70	7.57	3.17	0.58	0.12	7.11	98.08	2116	13	72	9	14	25	14	22	16.2	189	4.2	169	40	111
JB24	F lam sst	Bky	67.90	0.60	9.20	4.33	0.09	1.81	4.99	3.27	1.30	0.12	5.19	98.81	368	35	27	10	10	29	6	41	10.7	95	5.1	87	36	101
JB28	F msv sst	Bky	73.32	0.49	9.58	3.01	0.05	1.00	1.99	4.35	2.02	0.08	2.98	98.83	808	33	42	11	7	15	4	45	7.0	78	5.4	68	20	102
JB69	Msv slt	Kps	53.08	0.79	15.84	8.68	0.06	3.77	4.51	3.42	2.01	0.19	6.75	99.11	315	67	116	23	13	73	4	68	20.1	83	9.7	234	32	162
JB70	Msv slt	Kps	57.02	0.88	14.12	6.75	0.07	3.26	4.91	1.23	3.22	0.21	7.00	98.65	595	54	109	17	13	58	4	113	16.2	72	12.1	223	33	194
JB71	Msv slt	Kps	58.89	0.71	11.37	5.22	0.11	2.83	5.40	4.03	1.76	0.17	8.45	98.93	339	45	73	15	10	18	4	65	13.4	75	7.5	146	28	142
JB72	Msv slt	Kps	57.97	0.91	10.30	6.20	0.09	3.10	5.75	3.50	1.52	0.26	9.08	98.67	315	71	116	12	13	40	4	55	13.1	62	9.9	163	36	297
JB73	Msv slt	Lks	50.23	0.78	12.11	6.49	0.13	4.23	8.79	1.20	3.07	0.18	10.77	97.98	851	50	80	16	14	49	8	105	14.0	133	10.7	126	30	180
JB74	Crs msv sst	Lsw	57.28	0.79	10.66	5.00	0.10	2.48	8.19	0.68	2.78	0.20	9.82	97.98	646	81	72	14	14	34	4	125	13.0	339	9.9	123	51	238
Upper Likasi Formation (Ng 1.3)																												
JB38	F msv sst	Bky	62.84	1.70	10.04	7.52	0.11	3.01	3.13	3.78	0.39	0.14	4.30	96.97	786	42	140	14	17	43	5	15	25.0	125	3.9	236	33	141
JB63	Msv slt	Kps	54.36	0.81	15.54	7.94	0.10	4.06	3.62	2.10	2.98	0.20	7.12	99.04	426	58	126	22	13	66	4	100	19.8	40	8.1	265	32	162
JB64	Lam slt	Kps	56.57	0.87	14.49	7.31	0.10	3.79	3.72	2.32	2.56	0.21	7.29	99.23	349	60	112	20	12	64	4	89	17.5	48	9.0	216	33	177
JB65	Lam slt	Kps	55.71	0.72	12.22	6.34	0.12	3.32	6.08	2.60	1.90	0.17	9.13	98.93	260	50	93	16	11	63	4	67	13.8	75	8.3	163	29	148
JB66	Lam mst	Kps	56.42	0.88	16.30	7.60	0.08	3.71	2.58	2.37	2.98	0.21	6.20	99.30	377	73	124	23	14	69	4	100	20.4	35	10.3	266	33	177
JB68	Msv slt-lam mst	Kps	54.32	0.81	14.12	6.21	0.13	4.40	4.85	2.54	2.42	0.19	9.18	99.16	325	68	94	18	14	41	4	80	15.7	53	9.9	212	31	166
JB33	Lam slt	Bky	61.75	1.04	12.76	12.62	0.11	3.20	0.32	2.60	0.87	0.09	3.28	99.40	277	36	122	19	18	51	4	30	25.9	65	4.8	302	19	198
Grand Conglomerat (Ng 1.1)																												
JB51	F-vf msv sst	Kps	60.36	1.12	12.99	7.96	0.06	3.45	2.36	0.60	4.25	0.16	5.20	98.70	544	75	76	19	29	36	4	149	15.5	49	10.5	165	27	252
JB53	Vf msv sst	Kps	61.88	0.87	13.06	6.94	0.05	3.77	2.18	1.29	3.64	0.16	5.39	99.23	442	55	64	19	28	23	4	125	13.8	48	11.5	163	27	253
JB54	Vf msv sst	Kps	59.26	0.98	12.22	6.69	0.09	3.98	3.59	1.05	3.39	0.17	7.62	98.96	432	70	63	17	25	31	4	119	17.4	61	9.8	139	27	225
JB55	Vf msv sst	Kps	59.62	0.91	12.34	6.45	0.08	4.08	3.49	0.96	3.45	0.16	7.39	98.89	434	80	72	18	26	26	4	122	15.9	60	9.7	148	26	225
JB57	Vf msv sst	Kps	57.51	1.09	12.54	8.95	0.06	4.22	3.11	0.17	4.53	0.33	6.77	98.89	457	61	61	18	26	21	4	126	16.0	58	11.3	140	29	250
JB58	Vf msv sst	Kps	52.40	0.96	10.31	17.01	0.02	4.77	3.75	0.13	3.93	1.48	4.36	98.66	295	65	57	15	20	28	4	112	11.0	68	8.7	133	25	189
JB59	Vf msv sst	Kps	62.94	1.17	13.10	6.49	0.04	2.87	2.16	0.19	4.96	0.25	4.65	98.81	598	43	62	19	32	30	4	156	17.5	49	9.3	157	32	252
JB60	Msv slt	Kps	61.90	1.06	15.37	6.68	0.02	3.40	1.02	1.91	4.12	0.29	3.88	99.58	505	61	78	22	37	22	4	149	17.7	31	13.6	161	95	267

SaNr = sample number. Lith = Lithology (Crs- coarse; F-fine; Vf- very fine; msv- massive; Lam- laminated; sst- sandstone; slt- siltstone; mst- mudstone) Loc = locality (Bky- Bunkeya; Kps- Kipushi; Lks- Likasi; Lsw- Luiswishi; Tnk- Tenke).

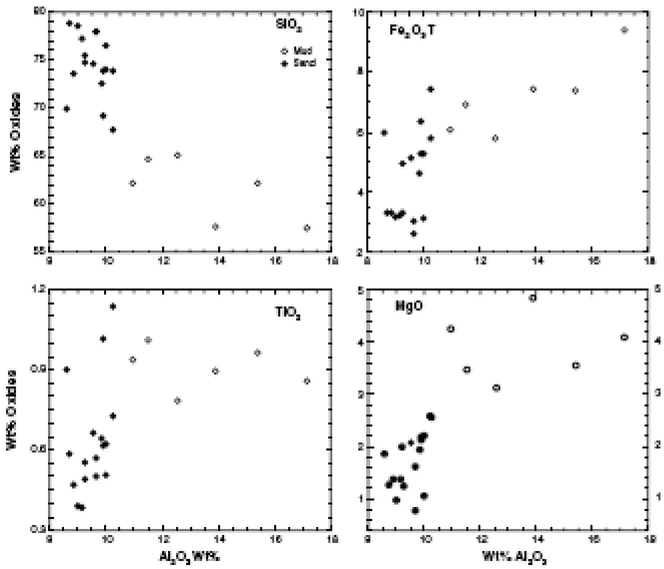

Fig. 6. Selected major element—Al_2O_3 variation diagrams for Monwezi Subgroup showing compositional difference between sandstones and mudrocks.

(Dickinson et al., 1983). However, Dickinson (1985) also notes that sands with similar compositions can also be derived from plutons exposed in deeply eroded magmatic arcs.

Nguba Group sandstones are characterized by a decrease of Lv/L and P/F ratios upward (Table 1), compatible with the general tendency of erosion to expose the deepest part of the basement or the roots of a volcanic province as time passes. Some support for derivation from a deeply dissected paleoarc source is given by Qp–Lv–Ls + m and Qm–P–K relations (Dickinson and Suczek, 1979; Dickinson, 1985). Although there is considerable scatter, most Upper Likasi and Monwezi sandstones have Qp–Lv–Ls + m relations that span arc orogen, mixed orogen, and collisional environments. However, Qm–P–K compositions are comparable with those of circum-Pacific volcanoplutonic suites (Fig. 9). The well-sorted nature of Plateaux Subgroup sandstones and their well-rounded quartz grains are suggestive of eolian deposition (e.g. Condie et al., 2001).

Composition of Nguba and Kundelungu Group rocks can be used to infer that of the source area as shown above that these sediments were deposited rapidly. Most Nguba and Kundelungu formations show an active margin affinities by falling within the active continental margin (ACM) field (Fig. 10(a)) and continental island arc (CIA) field (Fig. 10(b)). ACM field includes sediments derived from active continental margins or adjacent to active plate boundaries, and deposited in subduction-related basins, continental collision basins, and pull-apart basins associated with strike-slip fault zones (Roser and Korsch, 1986). Middle Kalule Formation samples are displaced into the arc field due to carbonate dilution, but have similar K_2O/Na_2O ratios to most other units. In contrast, most Upper Kalule and some "Grand Conglomérat" samples are displaced upward into the passive margin field, but with similar SiO_2 content. For the Upper Kalule Formation, this is most likely caused by a combination of weathering and K-metasomatism, as discussed below. In contrast, the higher ratios in the "Grand Conglomérat" are generated by lower Na_2O contents relative to the overlying units, whereas K_2O abundances are similar.

On Th–Sc–Zr discriminant (Fig. 10(b)), several Plateaux Subgroup samples fall within the passive margin field, and the remainder plot at the Zr apex. This may lend some support to its proposed eolian origin, with the relatively higher

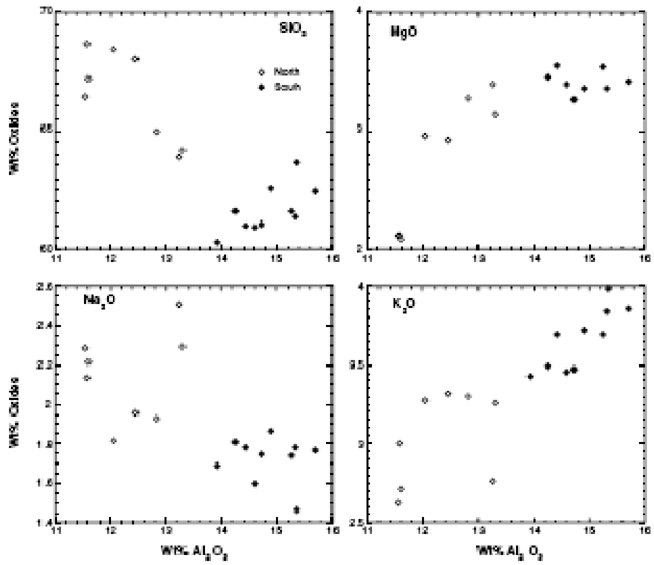

Fig. 7. Selected major element—Al_2O_3 variation diagrams for The "Petit Conglomérat" Formation showing north–south compositional difference.

Zr concentrations resulting from persistence of abrasion-resistant zircons. The distinction between CIA and ACM affinities reflected by these rocks (Fig. 10) is therefore not crucial here, the main point being that Th–Sc–Zr relations clearly indicate an active margin setting, rather than passive.

A relatively evolved margin and an evolved crustal source are indicated by the plot positions of average Proterozoic rocks (Condie, 1993) relative to the discriminant fields and the Likasi, Monwezi, and Kalule data (Fig. 10(b)). Average Neoproterozoic felsic volcanic rock (NPF) and Proterozoic TTG fall within the CIA field, near its lower edge and middle, respectively. Neoproterozoic basalt and andesite fall in the OIA field, and Proterozoic granite falls between ACM and PM. Although there is considerable overlap, Nguba Group and "Petit Conglomérat" samples are concentrated in the lower part of the CIA field near NPF, whilst Middle and Upper Kalule samples spread to higher Th above average Proterozoic TTG. This pattern also suggests that lower part of the succession had a slightly more mafic source than the upper part, as indicated by its higher Cr, Ni and V abundances. The more mafic content observed in the Nguba Group and Petit Conglomerat may be also related to the basaltic magmatism event during the Mwashia Subgroup deposition that is represented in the northern part of the Katangan belt by the Kibambale basalt (Kampunzu et al., 1991, 1993).

7.2. Source weathering

Nesbitt and Young (1982) introduced the Chemical Index of Alteration (CIA) to evaluate paleoweathering conditions. The index measures the extent to which fresh feldspars (CIA ≈ 50) have been converted to clays, but also permits estimation of average source composition in some instances. Application to the data here is limited due to excessive carbonate contents in many samples. Although this effect can be overcome by calculation of non-detrital carbonate contents and hence derivation of detrital CaO content (CaO*; Fedo et al., 1995), we lack the necessary CO_2 data. Consequently, we have confined CIA examination to samples with <3% CaO to reduce the impact of added carbonate.

The abundance of shales in the Nguba and Kundelungu Group successions shows that their sources were subjected to significant weathering. CIA values are low (up to ~60) in the Nguba Group (Fig. 11(a)). That and the presence

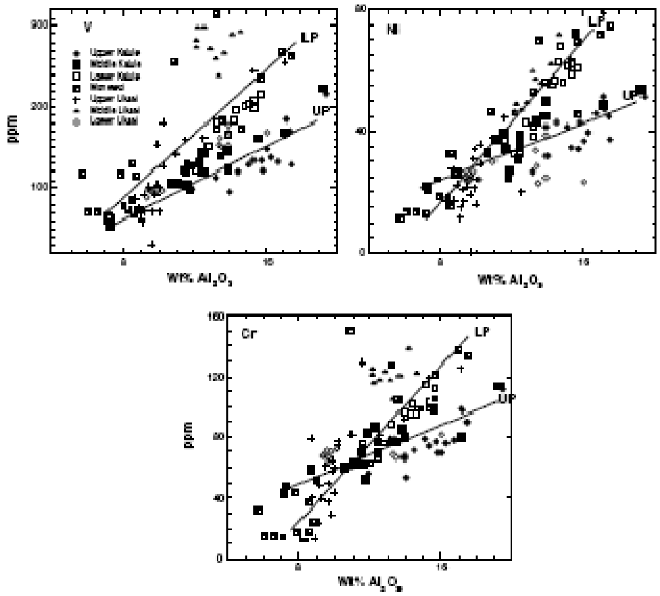

Fig. 8. Selected trace elements showing positive correlation with Al_2O_3 (anhydrous basis). Solid lines are illustrative detrital trends drawn by eye. UP: Upper part (Middle and Upper Likasi); LP: Lower part (Nguba Group and "Petit Conglomérat").

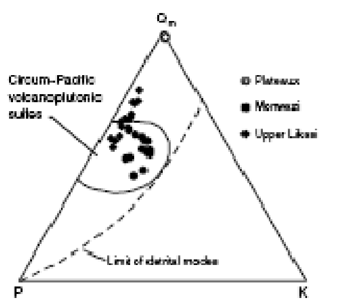

Fig. 9. Qm–P–K relations in sandstones from the Nguba and Kundelungu Groups, fields after Dickinson and Suczek (1979) and Dickinson (1985). Qm/P ratios increase in magmatic arc provenances below the Circum-Pacific field with increasing ratio of plutonic to volcanic sources, and increase above it due to increasing maturity in continental block provenances (Dickinson (1985)).

of immature sandstones containing relatively fresh detrital feldspars in Nguba rocks in the northern part of the Katangan belt point to a relatively unweathered or tectonically active source for this part of the succession. The "Petit Conglomérat" samples also have low CIA values (52–57). Only one Middle Kalule Formation siltstone has <5% CaO, and that also has low CIA (61). To circumvent the carbonate effect in this formation, we have also plotted an A–N–K diagram (Fig. 11(b)). This shows that the Middle Kalule samples plot near the field of the "Petit Conglomérat", suggesting similar weathering conditions prevailed at that time.

The low CIA (<63) values (Fig. 11(a)) and low Plagioclase Index of Alteration (PIA) values of the "Grand Conglomérat" and "Petit Conglomérat" samples with <5% CaO (46–68 and 51–59, respectively) are suggestive of a less weathered source, such as that interpreted to occur in frigid environments (Nesbitt and Young, 1982). These features, their textural immaturity, and the lack of linear inter-element correlations lend support to a glaciogenic origin for these two formations.

Upper Kalule samples plot well apart from the underlying formations in the A–CN–K diagram, falling in a tight group on the A–K join near the composition of muscovite (Fig. 11(a)), with nominal CIA values of 72–74. These values have almost certainly been influenced by post-depositional K-metasomatism (Fedo et al., 1995), and must originally have been much higher. As noted above, K_2O contents of the Upper Kalule samples are significantly greater than for the other units. On the A–CN–K diagram, ideal weathering trends should parallel the A–CN join when projected from potential source compositions, until the A–K join is reached (Nesbitt and Young, 1984). For the Nguba Group and the "Petit Conglomérat", ideal trends would form a zone extending between Proterozoic TTG and Proterozoic granite (Fig. 11(a)), representing the probable source composition. The effect of K-metasomatism is to displace samples towards the K-apex. However, this can be corrected by projection from the K-apex through the most aluminous sample in a given suite until its ideal weathering line is reached, thus yielding depositional CIA (Fedo et al., 1995). Because the Upper Kalule samples lie on the A–K join, original CIA values must have been at least 79–88, and may have been even higher (Fig. 11(a)). The paucity of Na_2O and CaO in the

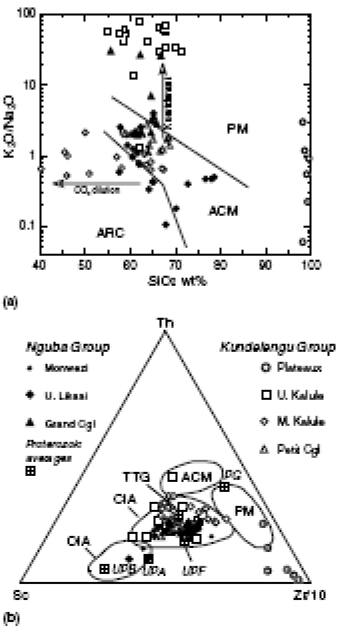

Fig. 10. Tectonic setting diagrams for the Nguba and Kundelungu Groups (a) SiO_2 versus K_2O/Na_2O (Roser and Korsch, 1986). PM: passive margin; ACM: active continental margin; ARC: arc setting. Arrows show shifts expected from carbonate dilution and K-metasomatism. (b) Th–Sc–Zr/10 (Bhatia and Crook, 1986). OIA: oceanic island arc; CIA: continental volcanic arc. Proterozoic rock averages from Condie (1993): PG: Proterozoic granite; TTG: Proterozoic Tonalite-Trondjhemite-Granite; NPF, NPA, and NPB are Neoproterozoic felsic volcanic rocks, andesites, and basalts, respectively.

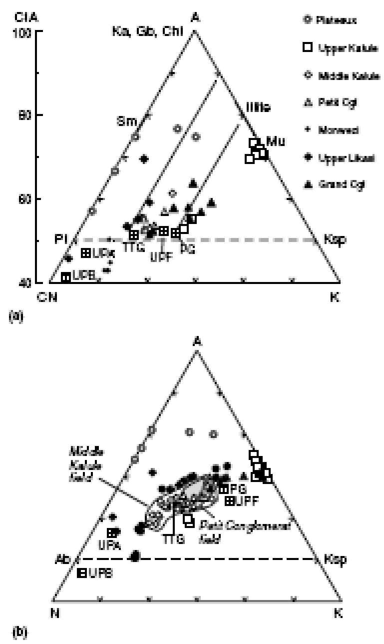

Fig. 11. (a) A–CN–K–K diagram (Nesbitt and Young, 1984) for Nguba and Kundelungu samples with <5 wt% CaO. A = Al_2O_3; CN = CaO + Na_2O; K = K_2O (molar proportions). Pl = plagioclase, Sm = smectite, Ka = kaolinite, Gb = gibbsite, Chl = chlorite, Mu = muscovite, Ksp = K-feldspar. Data are corrected for apatite but not calcite. Squares with crosses are Proterozoic rock averages from Condie (1993) as in Fig. 10(b). Solid lines from TTG and PG indicate the direction of ideal weathering trends from these protoliths. (b) A–N–K relations in the Middle Kalule Formation compared to the "Petit Conglomérat".

Upper Kalule Formation (Table 2) and very high Plagioclase Index of Alteration (PIA) values (Fedo et al., 1995) of 90–98 compared to the underlying units point to almost total destruction of plagioclase. The high CIA and PIA values of the Upper Kalule Formation suggest source area weathering was intense during its deposition, possibly under subtropical or tropical conditions (Nesbitt et al., 1997). The clustering of Upper Kalule data further suggest that they may have been derived from a source under "steady state" weathering conditions, during which erosion and weathering rates were comparable (Nesbitt et al., 1997). This suggests that tectonism in the Upper Kalule source was less active than in the underlying units.

As noted above, A-CN-K relations also have implications for tectonism. In a paper examining the stratigraphic position of the 'Roches Argilo-Talqueuses' (R.A.T.) in the Katangan Belt, Wendorff (2000) utilized K_2O–Na_2O and K_2O/Na_2O–Al_2O_3/Na_2O diagrams to examine relations between basement granites, and Roan and Kundelungu sediments in terms of weathering and recycling. He interpreted lower Na_2O in the Roan (except R.A.T.) and Kundelungu sediments compared to basement granitoids as representing the first cycle of erosion. Lower K_2O and similar Na_2O in the R.A.T. compared to the Roan sediments was interpreted as evidence for a second cycle. A K_2O–Na_2O plot for the data of this study shows that all units from the "Grand Conglomérat" through to the Middle Kalule have similar K_2O and Na_2O contents to the basement granites, and are quite distinct from the lower abundances in the underlying Roan succession (Fig. 12(a)). In contrast, Upper Kalule samples plot in the lower part of the Roan field and below. Plateaux samples are strongly depleted in both K_2O and Na_2O, and plot near the field of the R.A.T. However, on the K_2O/Na_2O–Al_2O_3/Na_2O diagram (Fig. 12(b)), all Nguba and Kundelungu samples lie along the curve of Roan sediments and basement granitoids from Wendorff (2000), suggesting common parentage but variable weathering.

The above features suggest that moderately weathered extrabasinal detritus was supplied to the Roan Group during initial extension, followed by fresher detritus in the Nguba Group, as derived from active basement uplift. Retention of similar Al–K–Na relations in the "Petit Conglomérat" and into the Middle Kalule Formation could reflect the basin inversion, which occurred at this time, which led to reduced influx of extrabasinal material and reworking of sediments from the Nguba Group itself. The increased CIA and clustering of data in the Upper Kalule Formation (Fig. 11) suggest subsequent reduction in tectonism and resumption of supply of weathered extrabasinal detritus similar to that provided to the Roan Group. In this context, the highly aluminous nature of the R.A.T. may simply reflect extreme in situ weathering of the Roan source, and first-cycle supply of that material to the initial basin fill of the Katangan Belt, rather than the polycyclic model proposed by Wendorff (2000).

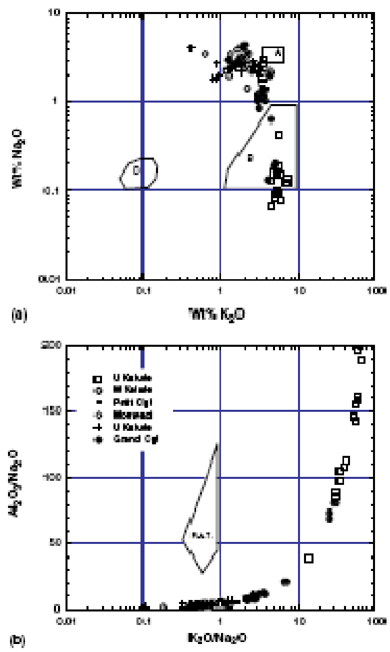

Fig. 12. (a) K_2O–Na_2O and (b) K_2O/Na_2O–Al_2O_3/Na_2O plots for the Nguba and Kundelungu Groups, compared to R.A.T, Roan and basement rocks, after Wendorff (2000). Fields on (a) from Wendorff (2000): (A) Basement granites; (B) Roan, Mwashia and Kundelungu argillites; (D) R.A.T.

7.3. Sediment provenance

As shown above, the Nguba Group and Kalule Subgroup rocks show inherited continental arc or active continental margin geochemical affinities (Fig. 10). An early Archaean source for the Nguba and Kundelungu Groups rocks is precluded, as virtually all samples fall within the post-Archaean field on the Ni–Cr plot (Fig. 13) of Taylor and McLennan (1985). However, a Neo-Archaean source remains possible. Many Neo-Archaean shales also fall within the post-Archaean field, even though others have higher Ni contents of 100–200 ppm, and fall outside it (Taylor and McLennan, 1985).

Cr/Th ratios have also been used to examine changes in source composition and crustal evolution, as major contrasts occur between Archaean and post-Archaean

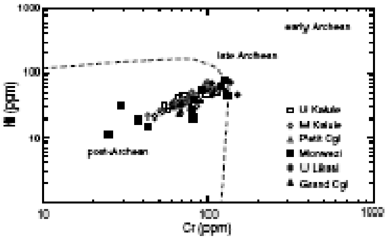

Fig. 13. Cr and Ni relationships in the Nguba and Kundelungu Groups. Fields after Taylor and McLennan (1985).

rocks (Condie and Wronkiewicz, 1990). Average Cr/Th ratios of the Nguba and Kundelungu Group formations range between 5.6 and 9.0, except for a somewhat greater average (17.4) in the Upper Likasi Formation. Ratios of <10 are typical of pelites deposited in the post-Archaean (<2.5 Ga), in contrast to the far greater ratios (10–300) exhibited by Archaean pelites (Condie and Wronkiewicz, 1990). Ratios in the Nguba and Kundelungu samples are comparable with 1.75–2.30 Ga pelites from the PWS (Pretoria–Waterburg–Southpansberg) trend of the Kaapvaal Craton in Southern Africa (Condie and Wronkiewicz, 1990). This similarity suggests that Proterozoic rocks formed the major part of the source for the Nguba and Kundelungu sediments, and any contribution from Archaean sources such as the adjacent Congo craton was minor.

As noted above, Nguba and Kundelungu samples with low CaO contents lie near the average compositions of Proterozoic TTG and Neoproterozoic felsic volcanic rocks, and spread as far as Proterozoic granite on the A–CN–K plot (Fig. 11(a)). This suggests the Nguba and Kundelungu sediments were derived from relatively felsic source rocks, and possibly of that age. However, this plot is not ideal for examining the differences between the groups, given the poor trends in individual formations and potential modification of the ratios of these mobile elements.

Immobile elements (e.g. Th, Sc, Zr, Ti) are more suitable for provenance determination, because they are more resistant to redistribution and are generally regarded as being transferred quantitatively from source to sediment (Taylor and McLennan, 1985; McLennan et al., 1993). When such elements are combined as ratios, the effects of carbonate dilution are overcome.

A Th/Sc–Zr/Sc diagram (McLennan et al., 1993) shows the Nguba Group samples have relatively small range in both Th/Sc and Zr/Sc ratios (Fig. 14(a)). The Nguba samples lie on a model source composition line linking the averages of Neoproterozoic basalt and Proterozoic granite, falling near TTG and NPF (Fig. 14(a)), confirming a relatively felsic source. Three Upper Likasi (JB38, 33) and Monwezi (JB21) samples, however, plot nearer Neoproterozoic andesite, suggestive of more mafic parentage. These samples are also enriched in ferromagnesian elements (TiO_2, Cr, Sc) relative to equivalents in each formation.

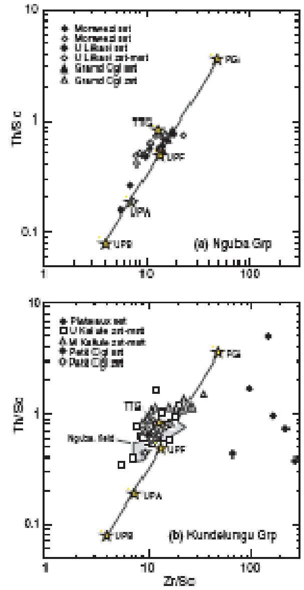

Fig. 14. Zr/Sc–Th/Sc diagrams (McLennan et al., 1993) for (a) Nguba and (b) Kundelungu Groups. Stars denote average compositions for Proterozoic rocks from Condie (1993). PG: Proterozoic granite; TTG: Proterozoic Tonalite-Trondjhemite-Granite; NPF, NPA, and NPB are Neoproterozoic felsic volcanic rock, andesite, and basalt, respectively. Inclined line between NPB and PG is an illustrative source composition trend. Field on (b) outlines the distribution of Nguba Group samples from (a), excluding the two samples plotting near NPA.

Most Kundelungu Group samples also plot on the source line (Fig. 14(b)), but tend to have higher values for both ratios. Although obscured on the plot, all "Petit Conglomérat" samples fall within the Nguba field. This is also compatible with derivation from underlying Nguba units exposed during inversion. Many Middle Kalule samples also fall within the Nguba field, but others spread to higher ratios, suggesting a slightly more felsic source. Plateaux Subgroup samples have extreme Zr/Sc ratios with similar Th/Sc ratios as the underlying Kundelungu units. Such increased Zr/Sc ratios at relatively constant Th/Sc are interpreted as a recycling effect (McLennan et al., 1993), due to relative concentration of resistant zircons, the main carrier of Zr, and destruction of less resistant Sc-bearing phases (e.g. pyroxenes, mafic rock fragments). Abrasion in an eolian environment would have much the same effect.

Similar patterns are shown by Ti/Zr and Ce/Sc ratios. Nguba Groups samples generally show little variation, with Ti/Zr ratios (20–34) and Ce/Sc ratios (2.5–6) similar to that of Proterozoic TTG. The three more mafic samples identified above have higher Ti/Zr (44–70) and lower Ce/Sc (0.8–1.8), again consistent with more mafic source. In the Kundelungu Group, "Petit Conglomérat" again has ratios identical to the Nguba Group, whereas Middle Kalule ratios spread toward higher ratios (up to 10), suggestive of a slightly more felsic source. Upper Kalule samples show greater range in Ce/Sc, with some samples falling to anomalously low values (near 1), but retain similar Ti/Zr ratios (20–35). The cause of these anomalously low Ce/Sc ratios is not yet clear, but may be due to Ce loss rather than more mafic source. With one exception, Plateaux Subgroup samples have very high Ce/Sc ratios (17–53) and very low Ti/Zr (2.3–4.5). These ratios are again understandable from the viewpoint of an eolian origin, suggesting survival of resistant heavy minerals such as monazite (Ce) and zircon (Zr).

The overall character of the sedimentary rocks analysed here and the small contrasts between formations outlined above can be summarized on multi-element diagrams after

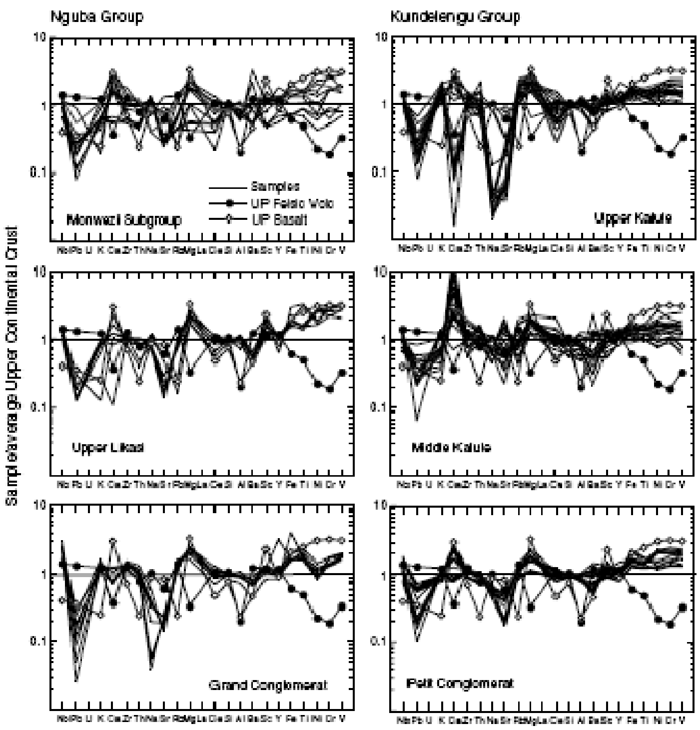

Fig. 15. Compositions of Nguba and Kundelungu Group rocks normalised against Upper Continental Crust (values of Taylor and McLennan, 1985), compared to the Neoproterozoic basalt (NPB) and felsic volcanic rock (NPF) averages of Condie (1993).

normalisation against average Upper Continental Crust (UCC). Average Neoproterozoic basalt and felsic volcanic rocks are also plotted for comparison (Fig. 15). The pattern for the "Grand Conglomérat" is relatively uniform despite its lithological variation, and abundances in the segment Rb–V are generally above UCC. This uniformity again lends support to a diamictite character. The pattern in the Upper Likasi Formation is similar, but is distinguished by uniformly greater abundances in the ferromagnesian element segment Fe-V, similar to average Neoproterozoic basalt, reflecting the slightly more mafic composition identified above. Some Monwezi Subgroup samples also show this enrichment, whereas others spread to values below UCC. This is largely a sorting effect, as the latter group rocks are mainly sandstones.

The patterns for the "Petit Conglomérat" are similar to those of the "Grand Conglomérat" and are also relatively uniform (Fig. 15). Middle Kalule patterns are disturbed by its carbonate content, with substantial enrichment in CaO in many samples. Abundances in the ferromagnesian segment Fe-V fall to below UCC, reflecting the slightly more felsic source proposed above. This may be more marked than apparent here, as all the Middle Kalule samples are mudrocks, which have less felsic compositions than sands derived from such sources. This pattern is repeated in the Upper Kalule Formation. Although mafic element contents increase slightly compared to the Lower Kalule, they are clearly less than in the Upper Likasi mudrocks. The other notable features of the Upper Kalule patterns are the marked depletion in CaO, Na_2O and Sr in most samples due to the intense weathering of its source, and enrichment in K_2O above UCC abundances due to K-metasomatism. As expected from its quartzose nature, Plateaux Group sandstones patterns (not illustrated) for all elements except SiO_2 are strongly depleted with respect to UCC, with abundances ranging from about 0.01–0.5 times crustal levels.

North to south lithological and petrographic changes in Nguba and Kundelungu Groups within the Katangan belt suggest that the Katangan basin opened to the south (Buffard, 1988; Batumike et al., 2002). The Paleoproteozoic Ubendian and the Mesoproterozoic Kibaride belts are exposed in the northern and northeastern parts of the Katangan belt. Both belts contain mafic and felsic igneous rocks displaying continental arc geochemical affinities (e.g. Andersen and Unrug, 1984; Kampunzu et al., 1985; Kapenda et al., 1998; Kokonyangi et al., 2004), and also contain lithologies similar to that of clasts recorded in the "Grand Conglomérat" and "Petit Conglomérat" (quartzite, granite, gneiss, rhyolite, mica schist, quartz: François, 1974; Batumike et al., 2002). The Ubendian and Kibaride belts thus comprise suitable sources for the rocks examined here.

In the southern district (e.g. Kipushi), the "Petit Conglomérat" displays higher contents of Al, Mg and Ca than that in the north (from Bunkeya), and its matrix is muddier than in the north, suggesting a more weathered source (e.g. ancient sedimentary suites) for the southern samples. This is also supported by the presence of intrabasinal clasts from the Roan and Nguba Groups in the south that are unknown further north, suggesting a southern provenance for the sediments in this area. This implies exhumation of the Nguba and Roan rocks at this time, and supports the interpretation that the "Petit Conglomérat" could mark the inversion from extensional to compressional tectonics during the evolution of the Katangan basin. The geochemical similarities between the "Petit Conglomérat" and the underlying Nguba units in general, as outlined above, also support this model.

The Meso- to Paleoproterozoic Irumides belt lies to the southeast of the study area, and contains mafic and felsic igneous rocks (Hanson et al., 1988; De Waele and Mapani, 2002). It thus could also be source for Katangan sediments. These inferences are also supported by Cr/Th ratios and the close match of the analysed samples with TTG and NPF compositions, suggesting that the bulk of the Nguba and Kundelungu Group detritus was derived from Proterozoic sources with active continental margin characteristics, and not from an Archaean source such as the Congo craton. A Proterozoic source is also indicated by a Paleoproterozoic age reported from detrital zircons in the Plateaux Subgroup (Master et al., 2002). However, additional geochemical, isotopic, and geochronological data are needed to test this interpretation.

8. Conclusions

The Katangan basin evolved from a wide rift basin to a foreland basin during deposition of the Nguba and Kundelungu Groups. Sediments were mainly derived from the north, with some contribution from the south. Although the source remained relatively felsic throughout, elemental abundances and ratios suggest a slightly more mafic source in the Nguba Group and the "Petit Conglomérat" than in the overlying units. QFL compositions and geochemical parameters indicate a basement uplift provenance, probably of Proterozoic age. Decreasing Lv/L ratios between the Upper Likasi and Monwezi Subgroup suggest stripping of partial volcanic cover and exposure of the roots of source terranes with continental arc geochemical affinities. The Paleoproterozoic Ubendian Belt, the Mesoproterozoic Kibaride and Irumide belts, and the Meso- to Paleoproterozoic Irumides are all potential sources for the Nguba and Kundelungu Groups sediments. Although interpretation is somewhat limited by carbonate contents, CIA ratios suggest source area weathering was generally moderate during deposition of the "Grand Conglomérat" through to the Middle Likasi Formation. Low CIA and PIA ratios and the relatively uniform chemical compositions of the "Grand Conglomérat" and the "Petit Conglomérat" lend some support to a cool or frigid climate and a glaciogenic origin for these units. Source weathering intensified during Upper Kalule deposition, when tropical or subtropical conditions may have prevailed, and tectonism lessened. The geochemical data are compatible with deposition of the Nguba Group in an extensional environment. Similar geochemical signatures in the "Petit Conglomérat" and perhaps the Middle Kalule Formation may reflect intrabasinal reworking of the Nguba Group during inversion, whereas geochemical contrasts in the Upper Kalule Formation may represent resumption of supply of extrabasinal detritus.

Acknowledgements

J.M.B. is grateful to the Japanese government for MEXT scholarship support and to the Geoscience Department of Shimane University for the use of facilities. The University of Lubumbashi, Gécamines and Forrest Mining Companies are thanked for field support. J. Kokonyangi is acknowledged for reading an early draft of the manuscript. This is part of an M.Sc. research by J.M.B. at Shimane University and Dr. Roser is thanked for supervision and advice. This is a contribution to IGCP-UNESCO 418 and 450 projects.

References

Andersen, L.S., Unrug, R., 1984. Geodynamic evolution of the Bangweulu Block, northern Zambia. Precambrian Research 25, 187–212.

Batumike, J.M., Cailteux, J., Kampunzu, A.B., 2002. Lithostratigraphy and petrography of Nguba and Kundelungu Groups, Katangan Supergroup, Katanga, D.R. Congo. In: 11th Quadrennial IAGOD Symposium and Geocongress 2002, 22–26 July 2002, Windhoek, Namibia, Extended Abstracts (CD-ROM).

Bellière, J., 1966. Les sédiments Kundelungiens dans l'Arc Mwashya—Bunkeya. Annales de la Société Géologique de Belgique 89, 357–373.

Bhatia, M.R., Crook, K.A.W., 1986. Trace element characteristics of graywackes and tectonic setting discrimination of sedimentary basins. Contribution to Mineralogy and Petrology 92, 181–193.

Buffard, R., 1988. Un rift intracontinental du Précambrien supérieur: Le Shaba méridional (Zaire). Doctorate Thesis, University of Maine, France, p. 316.

Cailteux, J., 1983. Le Roan shabien dans la région de Kambove (Shaba-Zaire). Etudes sédimentologique et métallogénique. Doctorate Thesis, University of Liège, Belgium, p. 232.

Cailteux, J.L.H., 2003. Proterozoic sediment-hosted base metal deposits of Western Gondwana, Abstract Volume of the Conference and Field Guidebook, In: 3rd IGCP-450 Meeting and Field Workshop, Lubumbashi, D.R. Congo, p. 223.

Cailteux, J., Binda, P.L., Katekesha, W.M., Kampunzu, A.B., Intiomale, M.M., Kapenda, D., Kaunda, C., Ngongo, K., Tshiauka, T., Wendorff, M., 1994. Lithostratigraphical correlation of the Neoproterozoic Roan Supergroup from Shaba (Zaire) and Zambia, in the central African copper-cobalt metallogenic province. In: Kampunzu, A.B., Lubala, R.T. (Eds.), Neoproterozoic Belts of Zambia, Zaire and Namibia. Journal of African Earth Sciences 19, 265–278.

Chabu, M., 1995. The geochemistry of phlogopite and chlorite from the Kipushi Zn–Pb–Cu deposit, Shaba, Zaire. Canadian Mineralogist 33, 1143–1152.

Condie, K.C., 1993. Chemical composition and evolution of the upper continental crust: contrasting results from surface samples and shales. Chemical Geology 104, 1–37.

Condie, K.C., Wronkiewicz, D.J., 1990. The Cr/Th ratio in Precambrian pelites from the Kaapvaal Craton as an index of craton evolution. Earth Planetary Sciences Letter 97, 256–267.

Condie, K.C., Lee, D., Farmer, G.L., 2001. Tectonic setting and provenance of the Neoproterozoic Uinta Mountain and Big Cottonwood groups, northern Utah: constraints from geochemistry, Nd isotopes and detrital modes. Sedimentary Geology 141–142, 443–464.

De Waele, B., Mapani, B., 2002. Geology and correlation of the central Irumide belt. Journal of African Earth Sciences 35, 385–397.

Dickinson, W.R., 1985. Interpreting provenance relations from detrital modes of sandstones. In: Zuffa, G.G. (Ed.), Provenance of Arenites. D. Reidel Publishing Company, pp. 333–361.

Dickinson, W.R., Suczek, C.A., 1979. Plate tectonics and sandstone compositions. American Association Petroleum Geologist Bulletin 93, 2164–2182.

Dickinson, W.R., Beard, L.S., Brakenridge, J.L., Erjavec, R.C., Ferguson, K.F., Knepp, R.A., Lindberg, F.A., Ryberg, P.T., 1983. Provenance of North American Phanerozoic sandstones in relation to tectonic setting. Geological Society of America Bulletin 94, 222–235.

Fedo, C.M., Nesbitt, H.W., Young, G.M., 1995. Unravelling the effects of potassium metasomatism in the sedimentary rocks and paleosols, with implications for paleoweathering conditions and provenance. Geology 23, 921–924.

François, A., 1973. Le niveau du calcaire de Kakontwe et ses faciès au Shaba. Académie Royale des Sciences d'Outre-Mer, Bulletin des Séances 1973-4, 844–861.

François, A., 1974. Stratigraphie, tectonique et minéralisations dans l'arc cuprifère du Shaba (Rép. du Zaïre). In: Bartholomé, P. (Ed), Gisements Stratiformes et Provinces Cuprifères. Centenaire Société Géologique de Belgique, Liège, 79–101.

François, A., 1987. Synthèse géologique sur l'arc cuprifère du Shaba (Rép. Du Zaire). Centenaire Société Belge de Géologie, pp.15–65.

François, A., 1995. Problèmes relatifs au Katanguien du Shaba. In: Wendorff, M., Tack, L. (Eds.), Late Proterozoic Belts in Central Africa. Musée Royal de l'Afrique Centrale, Tervuren, Belgique. Annales des Sciences Géologiques 101, 1–20.

Goddéris, Y., Donnadieu, Y., Nédélec, A., Dupré, B., Dessert, C., Grard, A., Ramstein, G., François, L.M., 2003. The Sturtian 'snowball' glaciation: fire and ice. Earth and Planetary Sciences Letters 211, 1–12.

Hanson, R.E., Wilson, T.J., Brueckner, H.K., Onstott, T.C., Wardlaw, M.S., Johns, C.C., Hardcastle, K.C., 1988. Reconnaissance geochronology, tectonothermal evolution, and regional significance of the middle Proterozoic Choma Kalomo block, southern Zambia. Precambrian Research 42, 39–61.

Intiomale, M.M., 1982. Le gisement Zn–Pb–Cu de Kipushi (Shaba, Zaire). Etude Geologique et Metallogénique. Doctoral Thesis, Université Catholique de Louvain, Belgium, p. 170.

Intiomale, M.M., Oosterbosch, R., 1974. Géologie et géochimie du gisement de Kipushi, Zaire. Centenaire Société Géologique de Belgique, Gisements stratiformes et Provinces cuprifères, 123–164.

John, T., Schenk, V., Mezger, K., Tembo, F., 2004. Timing and PT evolution of the whiteschist metamorphism in the Lufilian Arc-Zambezi Belt Orogen (Zambia): implications for the assembly of Gondwana. Journal of Petrology 112, 71–90.

Kampunzu, A.B., Cailteux, J., 1999. Tectonic evolution of the Lufilian arc (Central Africa Copperbelt) during the Neoproterozoic Pan-African orogenesis. In: Cox, R., Ashwal, L.D. (Eds.), Proterozoic Geology of Madagascar. Gondwana Research 2(3), 401–421.

Kampunzu, A.B., Kabengele, M., Kapenda, D., Rumvegeri, B.T., Tshimanga, K., 1985. Evolution géologique des chaînes Ubendienne et Kibarienne avec référence spéciale au magmatisme. Abstract 13th Colloquium African Geology, St. Andrews, Occasional Publication 1985/3, CIFEG, Paris, pp. 44–45.

Kampunzu, A.B., Kapenda, D., Manteka, B., 1991. Basic magmatism and geotectonic evolution of the Pan African belt in central Africa: evidence from the Katangan and West Congolian segments. Tectonophysics 190 (2–4), 363–371.

Kampunzu, A.B., Kanika, M., Kapenda, D., Tshimanga, K., 1993. Geochemistry and geotectonic evolution of late Proterozoic Katangan basic rocks from the Kibambale in central Shaba (Congo). Geologisch Rundschau 82, 619–630.

Kampunzu, A.B., Wendorff, M., Kruger, F.J., Intiomale, M.M., 1998. Pb isotopic ages of sediment-hosted Pb–Zn mineralisation in the Neoproterozoic Copperbelt of Zambia and Democratic Republic of Congo (ex-Zaire): re-evaluation and implications. Chroniques de Recherche Minière 530, 55–61.

Kampunzu, A.B., Tembo, F., Matheis, G., Kapenda, D., Huntsman-Mapila, P., 2000. Geochemistry and tectonic setting of mafic igneous units in the Neoproterozoic Katangan Basin, Central Africa: implication for Rodinia Break up. Gondwana Research 3 (2), 125–153.

Kampunzu, A.B., Moine, B., Bagai, Z., Cailteux, J.L.H., Loris, H.N.B.T., Ngoyi, K., 2002. Geochemistry of Neoproterozoic sedimentary rocks hosting stratiform copper, cobalt and nickel ore deposits in the Copperbelt of Central Africa (Congo and Zambia): metallogenic implications. In: 11th Quadrennial IAGOD Symposium and Geocongress 2002, 22–26 July 2002, Windhoek, Namibia, Extended Abstracts (CD-ROM).

Kampunzu, A.B., Cailteux, J.L.H., Moine, B., Loris, H.N.B.T., 2002. Geochemical characterization, provenance, source and depositional environment of 'Roches Argilo-Talqueuses' (R.A.T.) and Mines Subgroups sedimentary rocks in the Neoproterozoic Katangan Belt (Congo): Lithostratigraphic implications. In: 11th Quadrennial IAGOD Symposium and Geocongress 2002, 22–26 July 2002, Windhoek, Namibia, Extended Abstracts (CD-ROM).

Kampunzu, A.B., Cailteux, J.L.H., Batumike, J.M., Loris, N.B.T., 2003. Syn-orogenic sedimentation in the Katangan belt: myth or reality? Multi-proxy constraints. In: Cailteux, J.L.H. (Ed.), Proterozoic sediment-hosted base metal deposits of Western Gondwana (IGCP 450), 3rd Conference, Lubumbashi, Congo, Abstract volume, pp. 98–102.

Kapenda, D., Kampunzu, A.B., Cabanis, B., Namegabe, M., Tshimanga, K., 1998. Petrology and geochemistry of post-kinematic mafic rocks from the Paleoproterozoic Ubendian belt, NE Katanga (Democratic Republic of the Congo). Geologisch Rundschau 87, 345–362.

Key, R.M., Liyungu, A.K., Njamu, F.M., Somwe, V., Banda, J., Mosley, P.N., Armstrong, R.A., 2001. The western arm of the Lufilian Arc, NW Zambia and its potential for copper mineralization. Journal of African Earth Sciences 33 (3–4), 503–528.

Kimura, J.I., Yamada, Y., 1996. Evaluation of major and trace element analysis using a flux to sample ratio of two to one glass beads. Journal of Mineralogy and Petrology for Economic Development 91, 62–72.

Kokonyangi, J., Armstrong, R.A., Kampunzu, A.B., Yoshida, M., Okudaira, T., 2004. U-Pb zircon geochronology and petrology from Mitwaba (Katanga, Congo): implications for the evolution of the Mesoproterozoic Kibaride belt. Precambrian Research 132 (1–2), 79–106.

Loris, N.B.T., 1996. Etude des minéralisations uranifères du gisement cupro-cobaltifère de Luiswishi (Shaba, Zaïre): contextes géologiques et géochimiques. Discussion des modèles génétiques. Thèse de Doctorat en Sciences Appliquées, Polytechnic Faculty of Mons (Belgium), p. 374.

Master, S., Rainaud, C., Armstrong, R.A., Philips, D., Robb, L.J., 2002. Contribution to the geology and mineralization of the Central African Copperbelt: II. Neoproterozoic deposition of the Katangan Supergroup with implications for regional and global correlations. In: 11th Quadrennial IAGOD Symposium and Geocongress 2002, 22–26 July 2002, Windhoek, Namibia, Extended Abstracts (CD-ROM).

McLennan, S.M., Hemming, S., McDaniel, D.K., Hanson, G.N., 1993. Geochemical approaches to sedimentation, provenance, and tectonics. Geological Society of America Special Paper 284, 21–40.

Nesbitt, H.W., Young, G.M., 1982. Early Proterozoic climates and plate motions inferred from major element chemistry of lutites. Nature 299, 715–717.

Nesbitt, H.W., Young, G.M., 1984. Prediction of some weathering trends of plutonic and volcanic rocks based on thermodynamic and kinetic considerations. Geochimica and Cosmochimica Acta 48, 1523–1534.

Nesbitt, H.W., Young, G.M., McLennan, S.M., Keays, R.R., 1996. Effects of chemical weathering and sorting on the petrogenesis of siliciclastic sediments, with implications for provenance studies. Journal of Geology 104, 525–542.

Nesbitt, H.W., Fedo, C.M., Young, G.M., 1997. Quartz and feldspar stability, steady and non-steady-state weathering and petrogenesis of siliciclastic sands and muds. Journal of Geology 105, 173–191.

Porada, H., 1989. Pan-African rifting and orogenesis in southern to Equatorial Africa and Eastern Brazil. Precambrian Res. 44, 103–136.

Porada, H., Berhorst, V., 2000. Towards a new understanding of the Neoproterozoic-early Paleozoic Lufilian and northern Zambezi Belts in Zambia and the Democratic Republic of Congo. Journal of African Earth Sciences 30 (3), 727–771.

Roser, B.P., Korsch, R.J., 1986. Determination of tectonic setting of sandstone-mudstone suites using SiO_2 content and K_2O/Na_2O ratio. Journal of Geology 94, 635–650.

Roser, B.P., Korsch, R.J., 1988. Provenance signatures of sandstone-mudstone suites determined using discriminant function analysis of major-element data. Chemical Geology 67, 119–139.

Roser, B.P., Sawada, Y., Kabeto, K., 1998. Crushing performance and contamination trials of a tungsten carbide ring mill compared to agate grinding. Geoscience Reports of Shimane University 17, 1–11.

Taylor, S.R., McLennan, S.M., 1985. The Continental Crust: Its Composition and Evolution. An Examination of the Geochemical Record Preserved in Sedimentary Rocks. Blackwell Science Publications, p. 311.

Tembo, F., Kampunzu, A.B., Porada, H., 1999. Tholeiitic magmatism associated with continental rifting in the Lufilian Fold Belt of Zambia. Journal of African Earth Sciences 28, 403–425.

Wendorff, M., 2000. Revision of the stratigraphical position of the Roches Argilo-Talqueuses (R.A.T.) in the Neoproterozoic Katangan Belt, south Congo. Journal of African Earth Sciences 30, 717–726.

Young, G.M., 1995. Are Neoproterozoic glacial deposits preserved on the margins of Laurentia related to the fragmentation of two supercontinents? Geology 23, 153–156.

Young, G.M., 2002. Stratigraphic and tectonic settings of Proterozoic glaciogenic rocks and banded iron-formations: relevance to the snowball Earth debate. Journal of African Earth Sciences 35, 451–466.